PHYSICAL REVIEW B VOLUME 46, NUMBER 1 1 JULY 1992-I

Structure difference between *i* and *T* phases of Al-Cu-Co and Al-Cu-Fe observed by Mössbauer effect

M. Eibschütz, M. E. Lines, H. S. Chen, and F. A. Thiel
AT&T Bell Laboratories, Murray Hill, New Jersey 07974

(Received 22 July 1991)

Room-temperature Mössbauer spectra have been measured for icosahedral (*i*-phase) $Al_{65}Cu_{20}Fe_{15}$ and iron-doped decagonal (*T*-phase) $Al_{65}Cu_{15}Co_{20}$ quasicrystals. The observed *T*-phase spectrum is qualitatively different from any other known quasicrystal, and unquestionably demonstrates the presence of two quite separate distributions of iron sites in this phase. The results are interpreted in terms of an atomically decorated, prismatic Penrose-tile model of sufficient generality to cover a wide range both of binary and of ternary *T*-phase compositions. This same model is used to account for the absence of the "two-site" form of Mössbauer spectrum in *T*-phase Al-Mn compositions and to interpret the local structural features of *T* phases (as determined by extended x-ray-absorption fine structure) and their possible relationship to local *i*-phase environments.

The discovery of stable icosahedral (*i*-phase) and decagonal (*T*-phase) quasicrystals which possess x-ray-diffraction lines as sharp as those of the best conventional crystals has renewed efforts to determine the detailed atomic structures of these materials. As exemplified by $Al_{65}Cu_{20}Fe_{15}$ (*i* phase) (Ref. 1) and $Al_{65}Cu_{15}Co_{20}$ (*T* phase),[2,3] there is now a general recognition that they are, respectively, related in some manner to three- and two-dimensional assemblies of decorated Penrose tiles (PT's), although in neither case is the precise decoration of the tiles, nor even the precise arrangement of the tiles, settled beyond dispute.

Mössbauer quadrupole spectroscopy is, in general, a useful probe of local environment in any context. However, to date, the measurements on (iron-doped) Al-Mn quasicrystals[4–6] have been of little value in differentiating between *i*- and *T*-phase environments since all existing room-temperature (RT) spectra have been found to possess a qualitatively similar form, namely, a somewhat broadened single quadrupole doublet. In this Brief Report we report RT Mössbauer spectra for *i*-phase $Al_{65}Cu_{20}Fe_{15}$ and (iron-doped) *T*-phase $Al_{65}Cu_{15}Co_{20}$ and establish the existence of *qualitative* differences between them. In particular, the spectrum for the *T*-phase quasicrystal is *unquestionably* composed of two doublets and, therefore, establishes the existence of two quite distinct iron sites (or, more likely, narrow distributions of iron site) in this particular *T*-phase crystal. The *i* phase exhibits the single broad doublet spectral type observed in all earlier quasicrystal Mössbauer experiments.[4–9] After reporting the experimental details, we shall offer a possible explanation for the unusual *T*-phase spectrum in terms of a two-dimensional Penrose tiling of a specifically decorated prismatic PT. The model is also capable of predicting in which classes of *T* phase the one- and two-doublet spectra should be observed.

Alloys of $Al_{65}Cu_{20}Fe_{15}$ and $Al_{65}Cu_{15}Co_{20-x}Fe_x$ ($x = 0.1, 0.5$) were prepared by induction melting of high-purity Al, Cu, Co, and enriched ^{57}Fe in a boron nitride crucible under argon atmosphere. Ribbon samples of about 1 mm width and 30 μm thickness were obtained by melt spinning on a 20-cm-diam copper wheel rotating at 2000 rpm. X-ray-diffraction measurements confirm 100% icosahedral structure for $Al_{65}Cu_{20}Fe_{15}$ and decagonal structure for both iron-doped $Al_{65}Cu_{15}Co_{20}$ samples.

The ^{57}Fe Mössbauer absorption spectra were obtained in a standard transmission geometry with a ^{57}Co-in-Rh source. The resulting RT spectra for the *i* phase and $x = 0.5$ *T* phase are shown in Fig. 1. The $x = 0.1$ *T*-phase spectrum did not differ in any essential manner from that for $x = 0.5$. A zeroth-order fit using only isotropic Lorentzian quadrupole doublets [each defined by an isomer shift (Δ^{IS}) with respect to iron metal, a quadrupole splitting (Δ^{QS}), and a linewidth w] accounts for the essential features in each case (see Fig. 1). The *i*-phase fit requires only one such doublet, with $\Delta^{IS}, \Delta^{QS}, w = 0.22, 0.36, 0.36$ (all in units of mm/sec), while the *T*-phase fit requires two doublets with respective parameters $\Delta_1^{IS}, \Delta_1^{QS}$, $w_1 = 0.20, 0.31, 0.33$ and $\Delta_2^{IS}, \Delta_2^{QS}$, $w_2 = 0.14, 0.58, 0.33$, again in mm/sec.

Although virtually nothing is yet known of local environments in *T*-phase quasicrystals, there is now some consensus concerning local environments in *i*-phase Al-Mn quasicrystals. In the latter the MacKay icosahdron[10] (MI), which can itself be assembled from rhombohedral PT,[11] appears to be an essential building block.[12–14] The only significant counterclaim[15] probably results from an erroneous assumption that Fe and Cr together substitute randomly for Mn in these materials.[7] Although the precise manner in which the MI's pack together to form the *i* phase remains in dispute, the Mn atoms appear to occupy two distributions of sites associated, respectively, with "broken" or "unbroken" bonds[8] in the context of MI connectivity in crystalline α(Al-Mn-Si).[16] These "sites" are defined by cages of 10±1 Al atoms and appear to differ only in the mean nearest-neighbor (NN) distances involved, although these differences are smaller than seem to be readily discernible from extended x-ray-

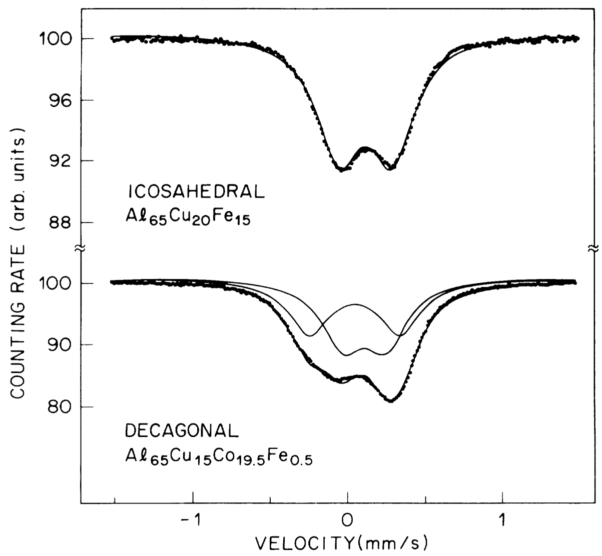

FIG. 1. Room-temperature iron Mössbauer quadrupole spectra for (a) *i*-phase $Al_{65}Cu_{20}Fe_{15}$ and (b) iron-doped *T*-phase $Al_{65}Cu_{15}Co_{20}$. The solid curves exhibit a lowest-order interpretation, respectively, in terms of a single and a pair of symmetric Lorentzian doublets.

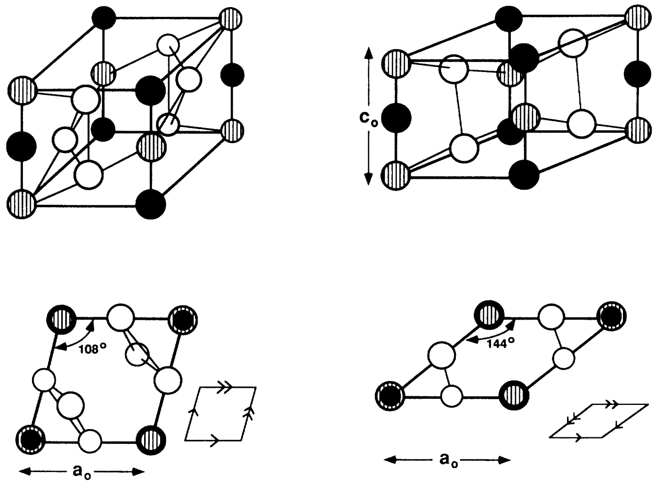

FIG. 2. Proposed atomic configuration of PT unit cells for Al-*M*-*M'* decagonal quasicrystals. The lower figures show *c*-axis projections and associated Penrose decoration as defined in Ref. 18. The open circles are Al atoms; the hatched and solid circles are the *s* and *s'* *M* "sites," which, however, are not fully occupied in any real quasicrystal and should not be uniquely associated with different *M* types.

absorption fine-structure (EXAFS) experiments. Their presence is deduced primarily by magnetic response (local moment stability), the substitution of Mn by smaller transition-metal (*M*) atoms (such as Fe and, presumably, Co) resulting in a preferential occupation of the smaller sites,[8] while substitution by larger transition metals *M* (such as Cr and V) results in a preferential occupation of the larger sites.[7]

Preferential occupation of different classes of quasicrystal site according to the size of the occupying atom seems therefore to be a well-established phenomenon in the quasicrystalline context. In particular, it provides a ready explanation of the existence of only one class of substituted Fe site and one broad Mössbauer doublet in the Al-Mn *i* phases. Since there is direct evidence[17] that *i*-phase Al-Mn and Al-Cu-Mn quasicrystals are structurally the same (in terms of their undecorated PT characterization), a parallel explanation may also be tenable for our observation of a single quadrupole doublet [Fig. 1(a)] for *i*-phase $Al_{65}Cu_{20}Fe_{15}$. Here, however, we wish to use this concept of preferential site occupation in the context of the far less studied *T* phase in an effort to interpret Fig. 1(b).

First, there is evidence[17] that both binary and ternary *T* phases are equivalent in their undecorated PT characterization, which we take to be stacked lattices of two-dimensional Penrose tilings. The known[2] ubiquitous presence, in the real-space structure, of Al pentagons stacked along the unique *c* axis with relative rotation of 36° leads us to propose the atomic PT decoration of Fig. 2. This is an embellishment of an earlier decoration[18] proposed for the composition Al_4Mn. It possesses two classes (*s* and *s'*) of non-Al site, neither of which is fully occupied in any actual *T* phase. We note that, once the Al decoration has been fixed, all other possible high-symmetry sites for *M* atoms can be ruled out since they give rise to unacceptably short Al-*M* bond lengths ≈ 1.7 Å.

Adopting, for simplicity and generality, a prismatic PT with linear dimensions $a_0 = c_0$ (in most Al-based *T* phases, $a_0 \lesssim c_0 \approx 4.2 \pm 0.1$ Å), we readily calculate the NN and next-nearest-neighbor (NNN) interatomic distances as follows:

$$\begin{aligned} &d_{\mathrm{NN}}(s\text{-}s') = 0.500a_0 \quad (c\text{-axis NN}) , \\ &d_{\mathrm{NN}}(\mathrm{Al}\text{-}s) = d_{\mathrm{NN}}(\mathrm{Al}\text{-}s') = 0.559a_0 , \\ &d_{\mathrm{NN}}(\mathrm{Al}\text{-}\mathrm{Al}) = 0.588a_0 , \qquad (1) \\ &d_{\mathrm{NN}}(s\text{-}s) = d_{\mathrm{NN}}(s'\text{-}s') = 0.618a_0 , \\ &d_{\mathrm{NNN}}(\mathrm{Al}\text{-}s) = d_{\mathrm{NNN}}(\mathrm{Al}\text{-}s') = 0.710a_0 . \end{aligned}$$

The only unphysically short value is that (≈ 2.1 Å) for the *c*-axis NN. It is this situation which precludes full occupation of *s* and *s'*, partial occupation relieving the situation via relaxation and, in all probability, playing a role in the determination of the various *c*-axis repeat distances observed in different *T* phases.[19]

When the PT's in Fig. 2 are assembled into a Penrose decagonal lattice, as depicted (for example) in Fig. 7 of Ref. 18, it is now a straightforward procedure to compute the complete set of local NN configurations (at distances $\le 0.71a_0 \lesssim 3$ Å), which may arise in the macroscopic lattice about the now topologically equivalent *s* and *s'* non-Al (i.e., *M*) sites. There are (ignoring any local relaxation effects) five different configurations: They are shown, together with their respective frequency f_i of occurrence[20] (with $\sum_i f_i = 1$) in Fig. 3. Labeling them $a-e$ [shown, respectively, in Figs. 3(a)–3(e)] in order of decreasing mean NN bond distance $\bar{d}$, we observe that they each possess a total of ten non-*c*-axis locations made up of three possible types: viz., a shorter Al bond [$d(\mathrm{Al}(1))$] at $0.559a_0$, a longer Al bond $[d(\mathrm{Al}(2))]$ at $0.710a_0$, and an intermediate-length M bond at $0.618a_0$. The five sites are characterized in terms of their respective non-z-axis coordination with numbers $n(\mathrm{Al}(1))$, $n(\mathrm{Al}(2))$, and $n(M)$ and their mean bond lengths $\bar{d}$ in Table I. To these coordination numbers should be added either zero or one z-axis M NN (a full two-coordination along the z axis being excluded for the bond-length reasons cited above).

Although EXAFS findings can be somewhat model biased, existing experimental evidence of this kind[21–23] does indicate (at least for many ternary compositions) that the *mean* M NN environment does not change drastically on passage from the i to T phase and that the larger M-atom type tends to adopt a coordination with $n(\mathrm{Al}(2))>n(\mathrm{Al}(1))$ that is different from that of the smaller M, for which $n(\mathrm{Al}(2))<n(\mathrm{Al}(1))$. The simplest explanation, within the model of this Brief Report, is that the larger M atom (e.g., Cu in $\mathrm{Al}_{65}\mathrm{Cu}_{15}\mathrm{Co}_{20}$) tends to occupy preferentially the largest site available, viz., site a in Table I, which is the only M site for which $n(\mathrm{Al}(2))>n(\mathrm{Al}(1))$. The other M is then distributed over the remaining M sites, probably in a nonuniform manner that reflects the relative size of the atom in question and sites available.

TABLE I. Number (n) and type [Al(1), Al(2), M; see text] of the non-c-axis NN atoms of an M site at the five different coordinations which occur in the T-phase Penrose-tile model of this Brief Report. Also shown is the mean NN "bond length" $\bar{d}$ (in units of Penrose-tile dimension a_0) both for the case of M sites empty and M sites filled.

M site	$n(\mathrm{Al}(1))$	$n(\mathrm{Al}(2))$	$n(M)$	$\bar{d}$ empty (filled)
a	3	6	1	0.660 (0.656)
b	4	4	2	0.634 (0.631)
c	6	4	0	0.619
d	7	2	1	0.593 (0.595)
e	10	0	0	0.559

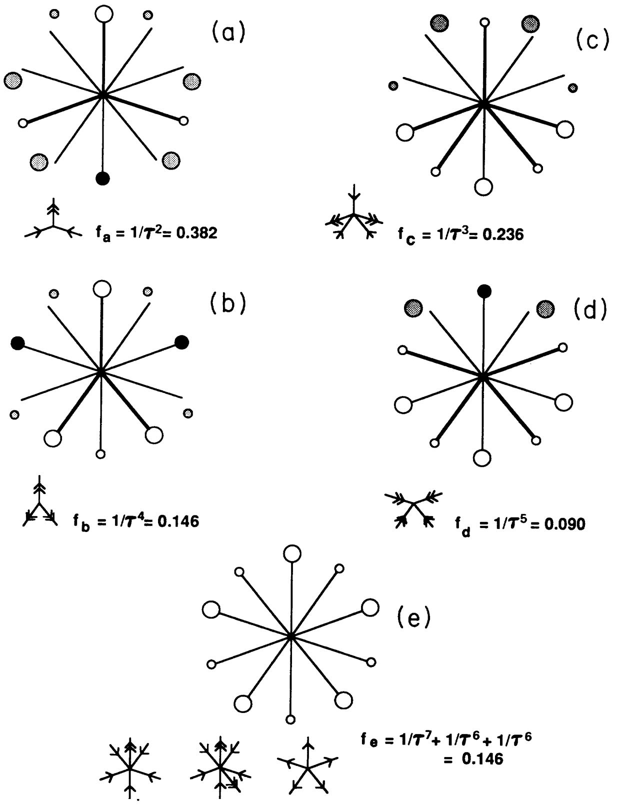

FIG. 3. Schematic of the five different types [(a)–(e)] of local NN environment for M atoms resulting from the decorated tiles of Fig. 2 in a complete Penrose lattice. Large (small) circles refer to Al atoms above (below) the plane of the paper, while solid circles refer to M atoms in the plane. The two types of Al bond lengths, short $[d(\mathrm{Al}(1))]$ and long $[d(\mathrm{Al}(2))]$ (see text), are denoted, respectively, by open and shaded circles. Also shown for each environment is an example of the class of generating PT diagrammatic vertex (see Ref. 18 for details) and the frequency f_i of occurrence of that NN environment in the full PT lattice [where $\tau=(\sqrt{5}+1)/2$].

Pursuing this model, we can find a qualitative explanation for many of the previously unexplained characteristics of the T phase, including the Mössbauer findings of this (and related) papers. First, from an examination of close-packed crystal structures,[24] combined with earlier Mössbauer, magnetic and EXAFS findings on quasicrystals, we anticipate a likely progression of M "atomic sizes" in the quasicrystalline context in the decreasing order

$$\mathrm{Sc}>\mathrm{Ti}>\mathrm{V}>\mathrm{Cr}>\mathrm{Cu}>\mathrm{Mn}>\mathrm{Fe}>\mathrm{Co}>\mathrm{Ni}\,. \tag{2}$$

We also note that a fractional population f of the total number of non-Al sites in Table I leads to a ternary quasicrystalline composition $\mathrm{Al}_{100-x}M_{x-y}M'_y$ in which

$$x=\frac{200f(1+\tau)}{2f(1+\tau)+2+4\tau}\,, \quad \text{with } \tau=(1+\sqrt{5})/2=1.618\ldots\,, \tag{3}$$

suggesting, in particular, that x must be less than 38.2 ($f=1$) for any viable T-phase composition.

Considering first the T-phase composition $\mathrm{Al}_{65}\mathrm{Cu}_{15}\mathrm{Co}_{20}$, we find that it can now be modeled closely by Cu fully (and uniquely) occupying sites a, whose site frequency is 0.382 (Fig. 3), and Co filling about 80% of the remaining smaller M sites b–e. When the a sites are filled, the solid circle M sites of Figs. 3(b) and Fig. 3(d) (which are always of type a) are also occupied, leading to a tenfold non-c-axis coordination at every M site except possibly at site a itself. If, however, the a sites are empty, then the M sites at b and d are also empty, leading to abnormally low coordinations at these sites. Such a low mean coordination has actually been observed[25] for Mn in T-phase $\mathrm{Al}_{78}\mathrm{Mn}_{22}$. We interpret this as a preferential occupation of sites b–d by Mn in this binary quasicrystal, the implied composition from Eq. (3) for full occupation of b–d being $\mathrm{Al}_{77.4}\mathrm{Mn}_{22.6}$.

The qualitatively different forms of the Fe Mössbauer spectra for iron-doped $\mathrm{Al}_{65}\mathrm{Cu}_{15}\mathrm{Co}_{20}$ [Fig. 1(b)] and T-phase $\mathrm{Al}_4\mathrm{Mn}$ (Refs. 4 and 26) are also explicable within the same model. For T-phase $\mathrm{Al}_4\mathrm{Mn}$, with sites a empty but sites b and c filled by Mn (theoretical composition $\mathrm{Al}_{80.9}\mathrm{Mn}_{19.1}$), we postulate that the smaller Fe atoms can preferentially occupy the smaller site *c*, but because of the abnormally low coordination of the *b* site in this context cannot readily enter the larger site *b*. The resulting single Fe site leads to a single Mössbauer quadrupole doublet spectrum. In *T*-phase $Al_{65}Cu_{15}Co_{20}$, on the other hand, the *a* sites are filled with Cu, leading to an increased coordination at site *b*. As a result, we postulate that Fe can now populate both sites *b* and *c*, leading to a two quadrupole doublet Mössbauer spectrum for this case. If, as seems likely, the lower-symmetry site *b* corresponds to the larger quadrupole splitting,[27] then the *i*-phase site [comparing Figs. 1(a) and 1(b)] would appear to possess an environment of higher symmetry—not unlike that of site *c*. We note, in particular, that the 6:4 ratio of short to long NN Al bonds at the *c* site corresponds rather closely to those $\approx 6{:}(4\pm1)$ reported[21–23,25] for the relevant *i*-phase *M* sites in a number of icosahedral quasicrystals.

Although our model thus far ignores details concerning local relaxation, layer stacking, and possible local *M* sublattice segregation effects between sites s and s', it is nonetheless clearly able to make crude predictions concerning the likely stability of the *T* phase as a function of composition. Clearly for example, the composition $Al_{65}Cu_{20}Fe_{15}$ is unstable as a *T* phase (if Cu can enter only the largest *M* sites) since it contains far more Cu than there are *a* sites available. As another example, we can consider Al-Co-Ni compositions. If, as seems probable, both Co and Ni are too small to occupy the *a* site, but with a relatively small a_0 value can occupy all the other sites (Co possibly favoring the larger and Ni the smaller), then the Al content of a stable Al-Co-Ni *T* phase should be close to $Al_{72}Co_{28-y}Ni_y$ (where we have used $f=1-0.382=0.618$ from Fig. 3). Actual stable Al-Co-Ni phases are found[3] near $Al_{70}Co_{30-y}Ni_y$, $10 \lesssim y \lesssim 15$.

In summary, we have observed a Mössbauer quadrupole spectrum in a quasicrystal which is qualitatively different from any other known and which requires the presence of two quite separate distributions of iron site for its interpretation. It is seen in iron-doped *T*-phase $Al_{65}Cu_{15}Co_{20}$ and can be explained in terms of an atomically decorated, prismatic Penrose-tile model of the decagonal quasicrystalline phase. This same model is able to account for the absence of a similar spectrum in the *T* phase of binary Al-Mn compositions and can also be used to account for EXAFS-determined local structural features of *T* phases and to suggest possible relationships between local NN coordinations in icosahedral and decagonal quasicrystals.

We thank A. Refic Kortan and M. A. Marcus for helpful discussions.

---

[1] A. P. Tsai, A. Inoue, and T. Masumoto, J. Mater. Sci. Lett. **6**, 1403 (1987); Jpn. J. Appl. Phys. **27**, L1587 (1988).

[2] A. R. Kortan, R. S. Becker, F. A. Thiel, and H. S. Chen, Phys. Rev. Lett. **64**, 200 (1990).

[3] A. P. Tsai, A. Inoue, and T. Masumoto, Mater. Trans. **30**, 463 (1989).

[4] B. Koopmans, P. J. Schurer, F. van der Woude, and P. Bronsveld, Solid State Commun. **59**, 619 (1986); Phys. Rev. B **35**, 3005 (1987).

[5] P. J. Schurer, B. Koopmans, and P. van der Woude, Phys. Rev. B **37**, 507 (1988).

[6] M. Eibschütz, H. S. Chen, and J. J. Hauser, Phys. Rev. Lett. **56**, 169 (1986).

[7] R. A. Dunlap, D. W. Lawther, and D. J. Lloyd, Phys. Rev. B **38**, 3649 (1988).

[8] M. Eibschutz, M. E. Lines, H. S. Chen, and J. V. Waszczak, Phys. Rev. Lett. **59**, 2443 (1987).

[9] Z. M. Stadnik and G. Stroink, Phys. Rev. B **38**, 10 447 (1988).

[10] A. L. MacKay, Acta Crystallogr. **15**, 916 (1962).

[11] V. Elser and C. L. Henley, Phys. Rev. Lett. **55**, 2883 (1985).

[12] Q. B. Yang, Philos. Mag. B **61**, 155 (1990).

[13] H. A. Fowler, A. J. Melmed, and H. B. Elswijk, Philos. Mag. B **61**, 811 (1990).

[14] Y. Ma and E. A. Stern, Phys. Rev. B **38**, 3754 (1988).

[15] C. Janot, J. M. Dubois, M. DeBoissieu, and J. Pannetier, Physica B **156&157**, 25 (1989), and references therein.

[16] M. Cooper and K. Robinson, Acta Crystallogr. **20**, 614 (1966).

[17] S. Ebalard and F. Spaepen, J. Mater. Res. **5**, 62 (1990).

[18] S. Takeuchi and K. Kimura, J. Phys. Soc. Jpn. **56**, 982 (1987).

[19] L. X. He, Y. K. Wu, and K. H. Kuo, J. Mater. Sci. Lett. **7**, 1284 (1988).

[20] V. Kumar, D. Sahoo, and G. Athithan, Phys. Rev. B **34**, 6924 (1986).

[21] A. Sadoc, Philos. Mag. Lett. **60**, 195 (1989).

[22] A. Sadoc and J. M. Dubois, J. Phys. Condens. Matter **1**, 4283 (1989).

[23] A. Sadoc, Philos. Mag. Lett. **60**, 21 (1989).

[24] R. W. G. Wyckoff, *Crystal Structures* (Krieger, Malabar, 1982), Vol. 1.

[25] F. Bridges, J. B. Bryce, G. M. Dimino, and B. C. Giessen, Phys. Rev. B **36**, 8973 (1987).

[26] R. A. Brand, G. LeCaer, and J. M. Dubois, J. Phys. Condens. Matter **2**, 6413 (1990).

[27] A simple NN model calculation, with one *c*-axis site occupied in each case and the same charge on each NN atom, gives a quadrupole splitting at site *b* approximately twice as large as at site *c*, in qualitative agreement with experiment.

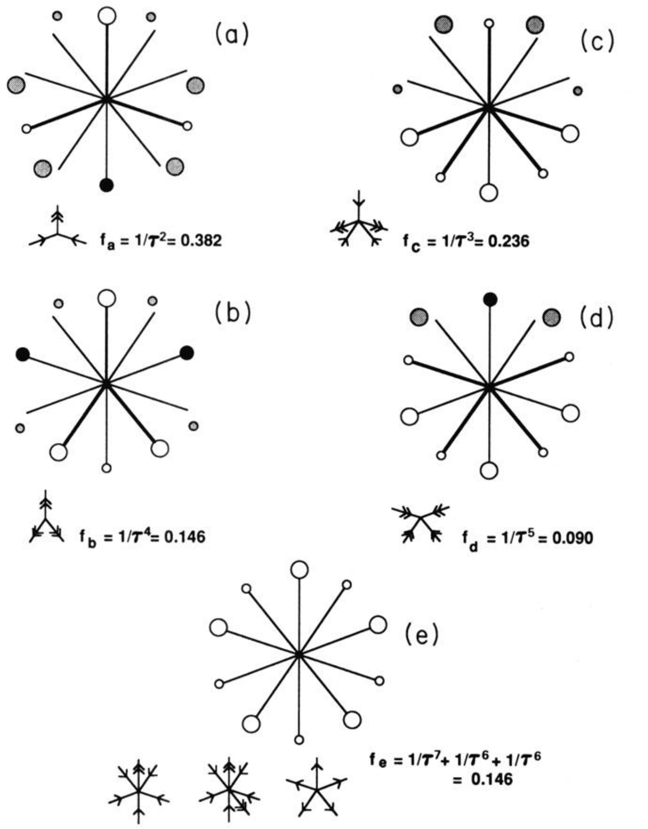

FIG. 3. Schematic of the five different types [(a)–(e)] of local NN environment for M atoms resulting from the decorated tiles of Fig. 2 in a complete Penrose lattice. Large (small) circles refer to Al atoms above (below) the plane of the paper, while solid circles refer to M atoms in the plane. The two types of Al bond lengths, short [$d(\mathrm{Al}(1))$] and long [$d(\mathrm{Al}(2))$] (see text), are denoted, respectively, by open and shaded circles. Also shown for each environment is an example of the class of generating PT diagrammatic vertex (see Ref. 18 for details) and the frequency f_i of occurrence of that NN environment in the full PT lattice [where $\tau=(\sqrt{5}+1)/2$].